Computers & Geosciences
October 2008, Volume 34, Issue 10, Pages 1338-1357
http://dx.doi.org/10.1016/j.cageo.2008.02.003

Response of the Rhône deltaic margin to loading and subsidence during the last climatic cycle

Gwenael Jouet[a, b, *], Eric W.H. Hutton[c], James P.M. Syvitski[c] and Serge Berné[a]

[a] Laboratoire Environnements Sédimentaires, Department of Géosciences Marines, IFREMER — French Research Institute for Exploitation of the Sea, Technopôle Brest-Iroise, BP 70, 29280 Plouzané, France
[b] Laboratoire CNRS UMR6538 Domaines Océaniques, Université de Bretagne Occidentale, IUEM, Place N. Copernic, Technopôle Brest-Iroise, 29280 Plouzané, France
[c] Environmental Computation and Imaging Facility, INSTAAR, University of Colorado, 1560 30th Street, Boulder, CO 80309-0450, USA

*: Corresponding author : Jouet G., email address : Gwenael.Jouet@ifremer.fr

Abstract:

Passive continental margin subsidence is initiated by the synrift mechanical stretching of the lithospheric upper brittle layer and continues during the postrift phase; the thermal cooling and contraction of the upwelled asthenosphere forces the margin to subside in addition to the overloads from sea water and sediments. Therefore, the total subsidence in stretched basins includes fault-controlled initial sinking, thermal subsidence and flexural isostatic compensations. Decoupling and estimating the different components of this subsidence from stratigraphic analysis and restricted geophysical and sedimentological databases remains problematic. In particular, backstripping the sediment layers requires a well-constrained geological framework. A method is proposed here to investigate the subsidence history of a margin based on forward stratigraphic modelling. Using the Sedflux model, several experiments are done using generally agreed upon assumptions on the parameters describing lithospheric rheology and isostatic behaviour of a margin. The stratigraphic modelling of the Rhône deltaic margin during the last climatic cycle (125 kyr) provides an assessment of these parameter estimates and their influence on geohistory (tectonic/thermal subsidence and sediment loading). The model results confirm the important impact of water loading on vertical deflection along the platform between glacial low sea-level and interglacial high sea-level. Based on Gulf of Lions (NW Mediterranean) observations, a conceptual method that uses the stratigraphic simulations is produced in order to evaluate the different components of the total subsidence of a margin, and, in particular, the relative impact of tectonic subsidence and sediment load.

Keywords: Subsidence; Isostasy; Stratigraphic simulations; Sedflux; Continental shelf; Gulf of Lions

1. Introduction

Present-day stratigraphic organisation and sedimentary thickness on a platform are products of cumulative changes in sedimentary systems through time. The location and preservation of depocentres, as shown by seismic profiles from the shelf, result from changes in accommodation. A significant subsidence rate of the margin is necessary to permit a continuous record and preservation of a depositional sequence. On passive margins, accommodation is most important at the shelf edge. The location and magnitude of the sediment sources, together with eustatic controls, may result in erosion of the sediment wedge on the inner shelf. Studying basin subsidence and sedimentary filling is essential for understanding the tectonic and thermal history of passive continental margins. Therefore, subsidence rate, together with sediment flux and global sea-level variations have to be taken into account in order to investigate the origin of vertical motions of marine continental shelves. Total subsidence, which contributes to accommodation, corresponds to medium to long-term Earth processes that involve constraints from lithospheric structure and asthenospheric cooling. The overloads of sediments and water amplify vertical movements, according to the laws of isostatic compensation. Numerous parameters are implied for this process. It is therefore difficult to disentangle and quantify the different components that contribute to the subsidence of the platform.

Geohistory analysis (Van Hinte, 1978), based on seismic stratigraphy and lithological information from boreholes or sediments cores, provides important constraints on the tectonic and/or thermal subsidence and sediment accumulation rates through time. Decompaction of the present-day sedimentary thicknesses, paleobathymetry and paleosealevel helps to evaluate the vertical evolution of a continental margin. Using this method, amounts of total and tectonic subsidence can be determined through decompaction of stratigraphy and backstripping of sediment load. This technique has been applied to investigate several margins worldwide (Ceramicola *et al*., 2005, Steckler *et al*., 1999). Watts and Ryan (1976) proposed the isolation of the tectonic driving force by removal of the isostatic effects of sediment load (i.e. the Backstripping technique). Unfortunately, the validity of the method requires a well-known sedimentary and structural system and precise estimates of specific parameters like compaction, paleobathymetry and absolute sea-level fluctuations. A quantitative analysis of subsidence rate through time relies on knowledge of basin formation and evolution.

There are two conceptual approaches to model a basin and to determine the factors that affect its formation and its infilling. The first is the backstripping method, which successively removes strata to recover a margin's geohistory. Most of the time, it is not simple to estimate each of the parameters required by this method. This leads to under- or over-estimation of the subsidence components. In particular, determination of paleobathymetry from observational data cannot generally be estimated with enough accuracy. In addition, the sediment record is discontinuous because of non-deposition and erosional events, and the complete geodynamic evolution of margins cannot be reconstructed (i.e. Bessis, 1986; Ceramicola *et al*., 2005, Steckler *et al*., 1999). Thus, backstripping implies assumptions about the geological evolution of the studied margin, without possibility for testing the validity of these hypotheses. The second approach, described here, uses forward stratigraphic modelling to simulate the delivery of sediment and its accumulation in a sedimentary basin (e.g. Syvitski and Hutton, 2001), and takes into account variations in the various controls on sedimentation. In conjunction with the backstripping method, the stratigraphic simulation is useful for investigating the boundary conditions of the evolution of a basin and its changes in accommodation.

This paper demonstrates the use of stratigraphic simulations to validate and extrapolate different hypotheses on basin dynamics and the formation of shelf sedimentary wedges. An estimate of subsidence and sediment thickness from seismic stratigraphic analysis is tested and refined during a simulation of the basin evolution. The method is applied to the Gulf of Lions as a case study. Next, a conceptual method using the stratigraphic simulations is produced to isolate the different components of total subsidence of a margin (tectonic/thermal subsidence, sediment and water loading) during a relatively short geological interval.

2. Subsidence and Isostasy

Sediment dispersion and deposition in a sedimentary basin is the product of the interplay between the generation of accommodation and sediment supply. Sediment accumulations and their internal geometries are therefore controlled largely by the tectonic/thermal and isostatic mechanisms that cause subsidence (Fig. 1). Change in accommodation is thus an important part of the driving mechanisms responsible for the stratigraphic pattern in basin-fill. If we consider a theoretical lithological column, these mechanisms can be subdivided into: 1- tectonic forcing controlling the spatial and temporal pattern of subsidence and the evolution of the sediment routing system, and 2- eustasy that essentially controls accommodation and sets base level (Allen and Allen, 2005). As a consequence, several vertical motions of the reference level can be observed (Fig. 1). Motions can be inferred from the evolution of each lithological unit and lead us to define the different components of the total subsidence (*S*). The lithospheric structural processes of margin formation and evolution through time are involved in the tectonic/thermal subsidence (*TS*), whereas global eustasy and sedimentation are associated and have an important impact on the isostatic response of this margin. Sea water defines the water loading (*WL*), which relies on sea-level variations. The thickness of sedimentary accretion is the result of erosion/deposition processes; it contributes to the sediment load (*SL*). We define "geohistory" subsidence (*GS*) as the combination of *TS* and *SL*. Seismic stratigraphy is one way to evaluate GS through time, often between two successive interglacial high sea-levels in order to remove the effects of sea-level variations. Below we discuss each component of the total subsidence and, in particular, the proportion of tectonic subsidence and sediment load in the geohistory subsidence (Fig. 2).

Insert Figure 1

2.1 Tectonic/thermal subsidence: basin formation

Our study focuses on the shelf area of passive continental margins (i.e. seismically inactive). In a uniform stretching model (McKenzie, 1978), the formation of a passive margin can be divided into two major phases of structural adjustments. During continental rifting, there is a brittle extension of the crust that produces the stretching of the continental lithosphere and a rapid synrift subsidence. After lithospheric thinning, a postrift phase is mainly governed by the cooling and contraction of the upwelled asthenosphere. The thermal relaxation is at the origin of an exponentially decreasing postrift subsidence. Synrift tectonic subsidence rates are typically <0.2 mm/y (200 m/My) and postrift tectonic subsidence rates are about <0.05 mm/y (50 m/My) (Allen and Allen, 2005). The amount of synrift and postrift subsidence depends essentially on the initial crustal to lithospheric thickness ratio and on the amount of stretching. The present-day tectonic/thermal subsidence of a margin is a long-term geological process that directly results from its structural and thermal context and history, and from its age (Fig. 1).

2.2 Isostatic subsidence

Increases in sediment load and water load causes additional subsidence of the sedimentary basin through the isostatic response of the lithosphere.

2.2.1 Subsidence from overload

Passive margins are characterized by seaward thickening prisms of marine sediments overlying a faulted basement of synrift sedimentary sequences. The postrift seaward-thickening sediment prisms consist predominantly of shallower marine deposits (Allen and Allen, 2005). This sedimentary wedge, together with the overlying sea water column modifies long-term tectonic subsidence. The weight of sediment deposited on a particular area of the shelf may cause the underlying crust to sink. Sediment erosion may cause the margin to rise.

A change in global sea-level relative to a reference datum is known as eustasy (Lisitzin, 1974). Eustasy in turn is one of the major causes of relative sea-level changes through hydro-isostasy (Johnston, 1995; Lambeck, 1997, 2000; Peltier, 2002; Posamentier *et al*., 1988), and thus impacts accommodation. Any increase (or decrease) of ocean volume must be compensated isostatically. Global sea-level changes are largely due to global climatic changes. As the earth’s climate cools, the ocean surface cools and ocean volume decreases (the steric effect). Additionally ice-sheets may form, storing water on land and reducing the ocean volume. During a warming period, ocean volume changes will move in the opposite direction. The major consequences of sea-level rise are observed at the glacial/interglacial transition, with differences between low and high sea-level positions of more than 120 m; between successive interglacial sea-level positions, the differences are minor.

2.2.2 Flexure of the lithosphere: isostatic compensation

Below some depth, there is no density contrast between two adjacent columns. The weight of the columns above this depth of compensation must be equal. This is a local isostatic balance (Airy, 1855; Pratt, 1855); the deflection of the crust at any location depends only on the local overload at that location (Airy and Pratt models of compensation). But the local isostatic balance neglects the lateral strength of the lithosphere and its relative rigidity. A more realistic model assumes that the lithosphere responds to loads like an elastic plate overlying an inviscid fluid (Kirby, 1983). Application of Archimedes principle suggests that bent continental plates are buoyed up by a force equal to the weight of the displaced mantle (Turcotte and Schubert, 1982). The net effect is for the entire region affected by flexure to be in regional isostatic balance. The lithosphere behaves approximately as an elastic beam of some assumed rigidity. A more rigid beam produces a broader and shallower deflection. A less rigid beam results in a deeper and narrower deflection.

A quantitative way to estimate the rigidity of the lithosphere is its effective elastic thickness (*EET*) (Burov and Diament, 1995; Watts, 1992).

$$EET = \sqrt[3]{\frac{12\left(1-v^2\right)D}{E}} \quad (1)$$

Two constants, the Poisson's ratio (v = 0.25) and the Young's modulus ($E = 7.10^{10}$ N/m^2), characterize the rheology (the stress/strain relationship) of the elastic portion of the crust and mantle lithosphere. D is the flexural rigidity in N/m. *EET* appears to be independent of the age of the load (Watts *et al*., 1982), which suggests that the elastic stresses that cause deflection, do not relax on a geological time scale. Adding a sediment and/or water load to the deflection causes the amount of deflection to increase. The most complete dataset currently available (Watts, 2001) describes values of *EET* between 5 and 110 km. For the specific application in the Gulf of Lions, Lambeck and Bard (2000) use an *EET* of 65 km in order to model the last deglacial isostatic rebound.

Using a simple model for bending a visco-elastic slab under a distributed load permits us to explore the effects of the isostatic components within a single-layer lithosphere. In the case of a glaciated margin, Huybrechts and De Wolde (1999) propose an isostatic ice-dynamic reconstruction model that assumes a rigid elastic lithosphere overlies a viscous asthenosphere. In this model bedrock adjustments are described by a single isostatic relaxation time. In this way, the isostatic compensation takes into account the effects of loading changes within an area several hundred kilometres wide. From this example, we obtain a value for the flexural rigidity (10^{25} Nm) corresponding to a lithospheric thickness of 115 km; the characteristic relaxation time for the asthenosphere is about 3,000 years (Huybrechts, 2002). The relaxation time is characteristic of the time dependence of the isostatic rebound process; it depends almost entirely upon the viscosity of the mantle. Relaxation times vary from approximately 3,400 years in SE Hudson Bay (Canada) to 4,200 years in the Gulf of Bothnia (Sweden) for postglacial rebound modelling (Peltier, 1998).

Thus, investigating the present-day stratigraphy should help us to estimate the accommodation history and evaluate the different components of subsidence that contribute to its changes. The typical response of continental stretching is early, rapid, fault-controlled subsidence followed by lithosphere cooling dominated by gravity-controlled deformation. Sediment accumulation and water load in a sedimentary basin causes extra-subsidence of the basement corresponding to a general basinward tilt in a long-term postrift tectonic and thermal subsiding context. The isostatic flexure of the lithosphere undergoing additional sedimentary load, such as a prograding sedimentary wedge, produces a regional deflection that is controlled by the effective elastic thickness of the lithosphere and the properties of the mantle viscosity (modelled by the relaxation time parameter). However, if the lithosphere reacts to the sediment load through regional flexure, the separation of the tectonic and sediment contributions is complex. The flexural loading of the sedimentary basin can be accounted for if the flexural rigidity and spatial distribution of the sediment load is known.

3. Methods for estimating subsidence

This study defines a method to better constrain the environmental and structural settings of a study area (Fig. 2), especially the isostatic behaviour of a continental shelf under different loading conditions (variations in sediment and water loads). There are different ways to estimate components of subsidence and to approach a margin's isostatic characteristics. The weakness of methods, such as "backstripping", is that they often require much knowledge about general settings that lead to many assumptions. In order to fix the isostatic parameters, one solution is to test them in their context and take advantage of stratigraphic simulations. Different hypothesis can be tested. Numerical stratigraphic models are useful for understanding the time-varying impact of sedimentary processes on the stratigraphic organisation. Stratigraphic simulation models are based on algorithms that conceptually or dynamically simulate the important input, boundary conditions and processes that define a sedimentary system (Syvitski, 1989). Subsidence, sea-level and isostasy combine to create accommodation in the basin, which controls sedimentation on the shelf. They also correspond to the main input values required for the simulations. In this way the different components of subsidence, measured during geohistory analysis, can be tested and estimated through numerical modelling.

Insert Figure 2

3.1 *Sedflux*: eustasy and subsidence modelling

Here, we apply the model *Sedflux (Hutton & Syvitski, this volume)* to simulate the delivery and accumulation of sediment within a basin through time. *Sedflux* includes the effects of sea-level and sediment supply fluctuations over time scales of tens of thousands of years. The basin-fill model allows for the continental margin to undergo tectonic processes (subsidence and uplift) and isostatic effects from sediment and water loads. The model architecture has a typical vertical resolution of 1 to 25 cm, and a typical horizontal resolution of 10 to 100 m. Various processes are modelled at a time step (days to years) that is sensitive to median-term variations of the seafloor (Syvitski and Hutton, 2001). A major subroutine of *Sedflux* corresponds to a momentum-driven hypopycnal plume, based on the Albertson *et al*. (1950) model of a submerged and steady, two-dimentional surface jet emanating out of a river mouth (Syvitski *et al*., 1998). This advection-diffusion subroutine introduces a time-varying sediment flux into the modelled basin to allow the stratigraphic organisation of sediment on a shelf. *Sedflux* requires as inputs an initial bathymetry of the basin at the simulation onset, and time-varying sediment flux and sea-level history. Of importance to this study are parameters related to subsidence and flexural response. In *Sedflux,* two different types of subsidence are considered: isostasy and tectonic subsidence. For isostatic subsidence, the lithosphere is treated as an elastic beam that is allowed to flex under the load of added sediment and water. For tectonic subsidence the user specifies subsidence rates at various positions and times (Syvitski and Hutton, 2001).

3.1.1 Tectonic subsidence

The physics of the processes that lead to tectonic or thermal movements are not modelled in *Sedflux*. Instead the results of these processes are incorporated as input to the model domain; vertical displacements for the modelled basin are specified in an input file, and these are allowed to vary both spatially and temporally. Subsidence and uplift rates are defined in meters per year at particular point along a basin for a specific instant in time. *Sedflux* interpolates these data to the defined temporal and spatial resolution of the particular model run. Results of the modelling provide confirmation of the range of subsidence rates used for it.

3.1.2 Isostatic subsidence

The changes in water and sediment load in a basin cause vertical lithospheric deflections (Fig. 1). In the case of a thick sedimentary wedge, subsidence becomes a leading process. *Sedflux* models subsidence due to loading using an elastic flexure model (Syvitski and Hutton, 2001). The elastic flexure model applied to Earth's crust makes four basic assumptions; 1- the lithosphere is assumed to have a linear elastic rheology, 2- the deflections are assumed to be small, 3- the elastic lithosphere is assumed to be thin compared to the horizontal dimensions of the plate, 4- planar sections within the plate are assumed to remain planar after deflection. For a single vertical load applied to the Earth's crust, the resulting displacements are given by:

$$w(x) = \frac{p(x)\alpha^3}{8D}\exp\left(-\frac{|x|}{\alpha}\right)\left(\cos\left(\frac{|x|}{\alpha}\right)+\sin\left(\frac{|x|}{\alpha}\right)\right) \qquad (2)$$

with α defined as

$$\alpha \equiv \sqrt[4]{\frac{4D}{\rho_m g}} \qquad (3)$$

and w is the displacement of crust due to sediment loading, D the flexural rigidity of the Earth's crust (i.e. Equ.1), ρ_m the density of the overlying sediment, and x the horizontal position. Because of our assumption of the linearity of our system, the resulting displacement due to multiple columns of sediment is simply the sum of the displacements due to each individual column.

After a load is applied, the viscous asthenosphere must flow out of the way before the lithosphere can deflect; causing a time delay between the addition of load and the lithosphere's response. Although models exist that predict the crustal response given a series of viscosity layers (Paulson *et al.*, 2005), this is beyond the scope of *Sedflux*. Instead, *Sedflux* assumes that the crustal response is exponential with time,

$$w(t) = w_0\left(1 - \exp\left(-\frac{t}{t_0}\right)\right) \qquad (4)$$

where w_0 is the equilibrium deflection as determined by Equation (2), t is the time since the load was applied, and t_0 is the response time of the lithosphere. The elastic flexure model in *Sedflux* only needs values for the effective elastic thickness (Equ.1) and the relaxation time (Equ.4) in order to calculate lithospheric deflections.

3.2 Method strategy

Based on the results from geohistory analysis (1 in Fig. 2), different parameters are used for several numerical runs of the stratigraphic model to estimate the different components of the total subsidence (S). The interpretation of seismic and lithological data allows the definition of the geohistory subsidence (*GS*) (2 in Fig. 2). The identification of dated erosion paleosurfaces permits us to quantify their vertical evolution through time and to estimate the

GS subsidence. This value takes into account both the tectonic subsidence (*TS*) and the loads due to sediment deposition (*SL*). Using the *GS* estimation and the sea-level variations as input parameters, the stratigraphic modelling can be realized with *Sedflux* (3 in Fig. 2).

The first stage of modelling is to experiment with different ranges of parameters that set the isostatic adjustment, in order to define of the best effective elastic thickness and relaxation time. The first model is run only with the *GS* subsidence (4 in Fig. 2), and provides a view of the tectonic subsidence added to the sediment load effect on the margin during the simulated time. The second model run does the same with eustasy (5 in Fig. 2). Therefore the margin responds to changing water load due to sea-level variations and consequently water column thickness fluctuates (*WL*). The combination of *GS* and eustasy is used for the third simulation (6 in Fig. 2), and corresponds to the modelling of the total subsidence (*S*) as all components are considered. These results are compared to the stratigraphic pattern observed on seismic profiles and parameters are adjusted in order to minimize the differences between model results and field observations (7 in Fig. 2).

The final stage of this method is to quantify the fraction of tectonic subsidence (*TS*) relative to the sediment load (*SL*) within the *GS* subsidence. For this simulation, a constant sediment flux is added to the *GS* subsidence and the eustasy, with the objective to reproduce the sedimentary thicknesses observed on seismic analysis (8 in Fig. 2). We call the resulting simulated subsidence *S'*, as it corresponds to the addition of total subsidence (*S*) with the sediment load (*SL*) (9 in Fig. 2). The comparison between *S* and *S'* allows us to estimate the effect of sediment load (*SL*) (10 in Fig. 2). Finally, the values of *SL* serve to partition *GS* subsidence into sediment load (*SL*) and tectonic/thermal subsidence (*TS*). Therefore, the suite of stratigraphic simulation provides an estimate of all the components controlling the vertical motion of the margin.

4. Application: Stratigraphic modelling of the Gulf of Lions margin

The subsidence history of the Gulf of Lions margin (Fig. 3) is investigated using stratigraphic simulations to calibrate our subsidence study. The available geophysical and lithological datasets provide an ideal well-constrained domain of application. Subsidence was historically explored on the basis of petroleum boreholes (Watts and Ryan, 1976) and multichannel seismic (Bessis, 1986; Bessis and Burrus, 1986). More recently, subsidence rate was established from high resolution seismic, constrained by modelling of the last 500 ky (Rabineau, 2001). Our method, using the *Sedflux* model, has been assessed for the last climatic cycle, and subsidence components have been estimated.

Insert Figure 3

4.1 Geological settings

The Palaeozoic and Mesozoic basement of the Gulf of Lions continental margin has undergone several phases of stretches and strains since the Hercynian orogeneses (Biju-Duval, 1984). The passive margin was shaped following the combined Oligo-Aquitanian rifting phase between continent and the Corsica-Sardinia microplate, and the Burdigalian crustal opening (Gueguen, 1995; Sioni, 1997). This margin is covered by sedimentary series dated from Oligocene to Quaternary (Bentounsi, 1990; Gorini *et al*., 1993). The synrift series (30-24 My) is topped by a Middle Aquitanian to Middle Burdigalian ravinement surface, which marked the onset of clastic postrift deposits. This depositional sequence (24-6.3 My) corresponds to the Miocene prograding wedge, largely eroded on the shelf and upper slope during the Messinian crisis (6.3-5.2 My) (Lofi *et al*., 2003). The upper Plio-Quaternary deposits have recorded the sedimentary structures associated with the increasing sea-level fluctuations during that time (Berné *et al*., 2002).

The Quaternary stratigraphic organisation of the Gulf of Lions is described by several conceptual models (Aloisi, 1986; Got, 1973; Monaco, 1971). High-resolution seismic data show, within the Middle and Late Quaternary, the repetition of several prograding wedges bounded by high amplitude seismic discontinuities (Fig. 4). These surfaces pinch out landward at about 80 m water depth. Within each seismic sequence, two major types of seismic facies are identified. Gently dipping clinoforms (PI) were interpreted as the product of mud deposition in a relatively low-energy environment whereas relatively high-angle clinoforms (PII, from 3° to 7°) were considered as corresponding to sandy upper shoreface facies (Berné *et al*., 1998; Gensous and Tesson, 1996; Rabineau, 2001; Rabineau *et al.* 2005; Tesson *et al*., 1990; Tesson *et al*., 2000). The major shelf sequences are associated with the Middle and Late Quaternary glacial/interglacial climatic and eustatic fluctuations. Regressive deposits constitute the majority of preserved sediments. Using stratigraphic modelling, Rabineau (2001) demonstrated that these sequences are linked to 100 ky orbital cycles.

Insert Figure 4

The present-day bathymetric configuration (Fig. 3) of the Gulf of Lions illustrates the present highstand situation with distinct lowstand, forced regressed and highstand systems tracts. The Holocene Rhône prodeltaic lobes and the last transgressive units, form the post-glacial subaqueous delta on the inner shelf, and sediment accumulations along the coast. From the middle to outer shelf, the majority of the prograding wedges correspond to regressive deposits. Parts of the wedges consist of muddy sedimentary bodies with gently dipping clinoforms while others form sandy shorefaces with high-angle clinoforms that settle on the outer shelf (Berné *et al*., 1998) (Fig. 5). This major seismic sequence, formed as a forced regression during the overall sea-level fall between MIS-3 and MIS-2, corresponds to a falling stage systems tract in the sense of Plint and Nummedal (2000). It can be sub-divided into several prograding units, which indicate that this relative sea-level fall was punctuated by intervals of increased or decreased falls, or even stillstand (Jouet *et al*., 2006). Major polygenetic regional erosion surfaces top the last two glacial sedimentary prisms. They formed both as subaerial and marine erosion surfaces during sea-level fall (sequence boundaries), and then were reworked (as a ravinement surface) during the ensuing transgression (Bassetti et al., 2006).

Insert Figure 5

The sequence deposited during the last climatic cycle is shown by a very-high resolution Chirp seismic profile (Fig. 5). It is located between the erosion surface *D60*, attributed to the penultimate glacial period (Marine Isotopic Stage 6 or MIS-6), and the erosion surface *D70*, formed during MIS-2 (Fig. 6). During glacial periods, sea-level was at a relatively low position, and favoured erosion. Although *D70* is defined as the last glacial erosion surface, we can observe it within an interglacial (highstand of sea-level, MIS-1) situation. Later in this paper, we will compare the present-day position (MIS-1) of *D70* to the position of *D60* (dated to MIS-6) at its subsequent interglacial position (MIS-5). For each case, it corresponds to the position of a glacial erosional surface at the following interglacial highstand.

4.2 Subsidence in the Gulf of Lions

During the Late Quaternary, the Gulf of Lions margin underwent postrift deformations. The amount of well-preserved sediment accumulation on the shelf attests to a considerable geohistory subsidence, which is the result of the combination of thermal subsidence and sediment load effects. The quantitative estimation of the geohistory subsidence in the Gulf of Lions was typically realised by the "Backstripping" method on depth converted seismic sections crossing the margin, and using several petroleum exploration boreholes (Bessis, 1986; Watts and Ryan, 1976). The variations of subsidence from the internal platform to the deep basin confirm the rapid initial burying of the margin between 30 to 23 My associated with crustal stretching during rifting (mechanic tectonic subsidence). The curves illustrate the exponential slowdown in postrift subsidence rate in response to the cooling of the lithosphere (thermal tectonic subsidence) without any significant tectonic activity. The cumulative subsidence of the basin (reaching 10 km in the deep basin) since the Oligocene would be equivalent to that calculated for older Atlantic margins (Bessis and Burrus, 1986; Burrus, 1984) although its age is only 30 My. Such magnitudes cannot be explained by an extensional model alone. The Gulf of Lions margin has the physiography of an Atlantic-type margin with the subsidence rate of an active margin (100-200 m/My) (Steckler and Watts, 1980). For the Upper Quaternary, Rabineau *et al*. (2005) estimates the geohistory subsidence rate at around 255 m/My at the shelf edge from the stratigraphic analysis of different seismic data sets and the modelling of cyclic stratigraphic sequences. It is based on the identification of dated erosion paleosurfaces that are interpreted as representing 100 ky glacial cycles (Fig. 5). The present position of the Messinian erosion surface is consistent with this value, and this work was used as a reference for estimating the vertical evolution of the margin (Fig. 6).

For the same period, Burrus and Audebert (1990) estimate the tectonic subsidence from about 20 m/My on the continental platform to about 180 m/My in the deep basin. The basic mechanism for postrift subsidence is thermal relaxation. However, according to Bessis and Burrus (1986), the loading effect of the sediment would contribute by 40 to 50 % to the total subsidence of the margin. Consequently, part of the high increase in accommodation could be due to the loading effect of sediments. The water loading effect was investigated by Lambeck and Bard (2000) on the basis of a comparison between observational evidence for sea-level changes along the French Mediterranean coast and the prediction from a glacio-hydro-isostatic model. From the last glacial period to present-day (Fig. 6), they tested the impact of the sea-level rise on the margin. A difference of 15 m between the position of sea-level during LGM and the present-day position of this paleoshoreline, confirms the importance of the isostatic rebound due to decreasing water column (Lambeck and Bard, 2000).

4.3 Results

Insert Table 1

Based on these estimates of the geohistory subsidence and using a compilation of global sea level from Waelbroeck *et al*. (2002) (Fig. 6), we ran several isostatic models with *Sedflux* for the last climatic cycle from 125 ky (MIS-5) to present-day (MIS-1) (Fig. 2). Models R1-R5 (Table 1) represent different isostatic adjustments obtained from the range of parameters tested and are broadly consistent with isostatic effective elastic thickness (*EET*) and relaxation time (*RT*), described in similar studies (sect. 4.2). The *EET* allows us to set local to regional flexural isostatic compensation and *RT* to fix slow to fast margin adjustments (Table 1). The geohistory subsidence (*GS*), used for simulation input, was defined as a progressive seaward tilt, taking into account the measured values of 255 m/My at 70 km from the coast (Rabineau, 2001). The convergence point of major seismic discontinuities roughly corresponds to the present shoreline (50 km on the simulated section). In a first approximation, this convergence point represents the position of the tectonic hinge point. However, its precise location cannot be determined geometrically because the magnitude of erosion affecting each surface is unknown. The sediment load (*SL*) effect is included in *GS*. Therefore, the R1-R5 Models were run without sediment input. Only the sea-level variations (*WL*) were added to *GS* in order to simulate the total subsidence (*S*). The simulation duration corresponds to the last 125 ky from the last interglacial and high sea-level to present warm period and highstand (Fig. 6). The strategy for these simulations is to compare the interglacial position of two successive erosional surfaces formed during two successive glacial low sea-levels.

Insert Figure 6

The seismic discontinuity *D70* (formed during MIS-2) is presently observed at the position that corresponds to interglacial MIS-1. *D70* is used as the initial surface for the simulation. We make the assumption that this surface represents the closest position that was occupied by the previous seismic discontinuity *D60* (formed at the penultimate glacial period MIS-6) during the last interglacial MIS-5 (125 ky). The final surface at the simulation end is compared with the present-day position of *D60* on seismic profiles. Otherwise, as described on seismic profiles, sandy wedges with high-angle clinoforms are preserved on the outer shelf and represent successive glacial shorefaces that can be used as a “dipstick” for sea-levels. It must be noted that the magnitude of erosion of these deposits was different during the last two glacial cycles; the last glacial sandy shoreface being better preserved compared to the shoreface formed during MIS-6 (Fig. 6). Nevertheless, the adjustment of the final simulated surface, based on these features, is feasible.

4.3.1 Test of rheology

The results of different tests on the lithosperic and asthenospheric behaviour are presented in figure 7. For each isostatic parameter (*EET* and *RT*) and for different values of them, the initial and final surfaces are plotted. Figure 7 shows, successively, the initial surface at the high sea-level of simulation onset (125 ky), the position of this surface during glacial low sea level, and finally, the simulated final surface at present-day position. The last erosional surface is compared with the present-day position of *D60* observed on the seismic profile (Fig. 5) and reported in this graph.

Insert Figure 7

We tested *EET* ranging from 50 to 100 km. Our results show that this value has relatively limited impact on the position of the final observed surface (Fig. 7). Only a difference in the isostatic response during the glacial period can be observed. In contrast, large variations of the position of final surfaces on the basis of different *RT* confirm the importance of this semi-empirical parameter, controlled by upper mantle cooling (sect. 2.2.2). The difference between the simulated and observed final position of *D60* is associated with the morphological difference between *D70*, used as the initial surface, and *D60*, the modelled surface (Fig. 7). The comparison is made to sandy paleoshorefaces that mark the paleoshoreline position through time. There is a good match between the simulated and observed paleoshoreline, except for differences in erosion. At this stage, the simulations do not take this erosion into account. From these tests, the preferred isostatic adjustment R8, for the following simulations, use an effective elastic thickness of 65 km and a relaxation time of 3,500 years (Table 1). The seismic interpretation otherwise leads us to run different scenarios of the geohistory subsidence. In particular, the seaward migration of the convergence point between *D70* and *D60* from 50 to 80 km provides a best fit between simulated and observed final surfaces between 70 and 90 km on the working section. Note that above this point, simulations are not precisely constrained. Only the marine part of the model is accurate enough for simulating the vertical motions.

4.3.2 Evolution of the total subsidence through time

Stratigraphic modelling points to a specific position along the section through the 125 ky of simulations. We observed, in particular, the evolution of the elevation at 100 km, where the total subsidence (*S*) variations can be quantified (Fig. 8). Simulations have taken into account only the geohistory subsidence (*GS*) or the water loading (*WL*) effect. Therefore, *S*, *WL* and *GS* are plotted as a function of simulated time and the difference of evolutions can be monitored (Fig. 8). The modelling confirms that the simple addition of *WL* and *GS* is not sufficient to reproduce the total subsidence. The evolution of each component of subsidence is dependant on the others. In particular, the water loading is mainly the consequence of relative sea-level, which is partly dependant on the geohistory subsidence (Fig. 1). The second aspect, deduced from these observations, is to consider the rapid total subsidence variations as the results of the water loading fluctuations. The *GS* is assumed to be constant along the simulations; the sea-level oscillations are the only parameter that can modify the load on the shelf. As a result, total subsidence mimics the seal-level variations of the last climatic cycle (Fig. 8.2).

Insert Figure 8

4.3.3 The geohistory subsidence and water loading effect

We estimate the importance of water loading on the vertical evolution of the shelf. From the tests described in figure 7, the platform is uplifted as sea-level falls until the glacial period (21 ky) even with geohistory subsidence active. Confirmation is seen in the results from the adapted isostatic model R8 (Fig. 8); the elevation, which only takes into account water loading, rises between 125 and 21 ky and then rapidly drops after the Glacial period when relatively low sea-level unloads the shelf. The impact of the *WL* on the shelf, between the glacial sea-level lowstand (21 ky) and the present-day highstand, can cause isostatic sinking of about 20 m at 100 km on the simulated section (Fig. 8).

Similarly the progressive sinking of the margin due to the combination of the tectonic/thermal subsidence and the sediment loading (*GS*) is estimated to be about 15 m for the last climatic cycle and about 5 m for the last deglaciation (from 21 ky to present-day).

4.3.4 Estimation of the sediment loading effect

Tectonic/thermal subsidence and sediment loading both contribute to the *GS*, which has been evaluated as 15 m of subsidence during the last climatic cycle (Fig. 8). During the stratigraphic model simulation R8, the sediment load contribution is taken into account in the *GS*, as we did not add sediment into the model domain. In order to estimate the contribution of sediment load into the *GS*, the model R9 was run with a sediment source (Table 1). The amount of sediment input was determined in order to obtain a sedimentary thickness equivalent to that measured on the seismic interpretation.

For this study, we considered the sediment influx as a constant parameter during the 125 ky; locally, the change in accommodation and the sediment load could suffer from this hypothesis, but the isostatic model, used to simulate the behaviour of the margin, is a regional flexural model and local loads do not have a significant impact on the isostatic response. Moreover, the modelled sedimentary thickness allows us to compare and to adjust the seafloor from seismic data and simulations at the top of this wedge.

Because sediment load is already included in the *GS*, model R9 calculates the final position of the erosion surface with twice the sediment load; one with the *GS* estimate and one with an imposed sediment flux. The final result allows us to present the simulated *D60* (with 2.*SL*) and the simulated *D70*, as we modelled the sedimentary thickness between these two major erosion surfaces (Fig. 9). The difference between simulated *D60* from R8 (*SL* is comprised in *GS*) and from R9 (2x*SL*) provides about 5 more meters of total subsidence (*S*+*SL*) at the end of the last climatic cycle simulation (Fig. 9), compared to the previous R8 total subsidence (*S*). It is mainly from the added *SL* contribution. If we now consider the 15 m of *GS* for the last climatic cycle, we can infer about 10 m of sinking related to the tectonic and thermal subsidence. Consequently, and from these 125 ky simulations, about 1/3 of GS is a result of sediment load (*SL*), while the remaining 2/3 is due to thermal subsidence (*TS*).

Insert Figure 9

4.4 Discussion

Successive low sea-level during glacial periods and their corresponding erosional surfaces have a cyclic repetition through time in the Gulf of Lions. Using these surfaces as chrono-stratigraphic indicators, it is possible to estimate the geohistory subsidence (*GS*) and the stratigraphic simulations of the last climatic cycle. In the *Sedflux* model, the flexural isostatic adjustments and compensation were simulated using parameters that are broadly consistent with isostatic effective elastic thickness (*EET*) and relaxation time (*RT*) described in similar studies (Huybrechts, 2002; Lambeck and Bard, 2000; Peltier, 1998; Watts, 2001). The high values of *EET* used for these experiments can be compared to the global bi-modal distribution of continental *EET* values established by Watts (1992). The 65 km effective elastic thickness corresponds to the lower part of Watts' distribution, that describes basins generally developed on high *EET* cratonic interiors. This value is in agreement with the geological setting of the structural region; the Gulf of Lions is a passive margin originating from Alpine thrust and its lithospheric thickness results from a long and complex marine and continental geological history.

Insert Table 2

From the simulations, we estimate each component of the total subsidence (*S*) (Table 2 and Fig. 9). First, the water loading (*WL*), associated with relative sea-level variations, can impact the vertical evolution of the margin between glacial lowstand and interglacial highstand. The range of *WL* effect can reach about 20 m. As a consequence, the position of glacial sedimentary features, observed at the present-day outer shelf, have to be corrected from this subsidence in order to approach the real water depth of their formation. For instance, Lambeck and Bard. (2000) determined a 15 m isostatic rebound for the last deglaciation period in the Gulf of Lions, as compared to our value of 20 m. Second, the geohistory subsidence (*GS*) measured on seismic is confirmed. The thermal cooling effect (*TS*) of the margin would contribute to about 60 to 65 % of the *GS*; the remaining fraction being represented by the sediment load (*SL*). These estimates are similar to those defined by Bessis and Burrus (1986). They are in the same range as estimates for other areas found in the literature (sect. 4.2) (Fig. 2). These comparisons demonstrate that our method provides, for short time-periods, results in the same range as those obtained through traditional approaches for longer time-scales. It allows one to take into account the hydro-isostatic effect, which is a key parameter for studying the impact of Quaternary glacial-interglacial sea-level changes. Moreover, our simulations confirm that the first order controls on depositional patterns are sea-level change and sediment supply, but that accommodation determines what is preserved in the Quaternary stratigraphic record.

5. Conclusion

Subsidence corresponds to the movement of the Earth's surface with respect to a reference level. Total subsidence has two major components: a tectonic part (mechanic and thermal) and a gravity part (sedimentary and hydrostatic loading). The aim of our method allows each of these components to be evaluated from a combined field stratigraphic and modelling approach. One application of the method is to estimate the impacts of global sea-level changes for a site where relative sea-level changes are stratigraphically well-constrained. The amplitudes of global Quaternary sea-level oscillations, derived from paleoclimatic proxies obtained from ice or sediment cores, need to be calibrated by independent geological measurements. On passive margins, the shelf edge is the place where accommodation is most important and direct measurement of successive relative sea-level positions is possible from the stratigraphic record (Jouet *et al*., 2006; Rabineau *et al*., 2005; Skene et al., 1998). The only way to evaluate absolute sea-level positions is to estimate the subsidence and correct the local eustatic curve. With new estimates of geohistory subsidence (*GS*) and global sea-level variations, stratigraphic simulations are adapted to understand the impact of water and sediment loading (*WL* and *SL*) on the shelf. Their rapid fluctuations (100 ky cycles) are superimposed on an overall trend corresponding to thermal cooling (*TS*) of the continental margin. This tectonic subsidence is a portion of the vertical deflection of the Earth's surface through time due to basin formation.

The stratigraphic modelling of the Rhône deltaic margin during the last climatic cycle (125 ky) allows the assessment of parameters estimated with the geohistory analysis (tectonic/thermal subsidence and sediment loading). Global eustasy fluctuations using the *Sedflux* model provides confirmation of the important impact of water loading on vertical motions of the platform between glacial low sea level and interglacial high sea level. Finally, the thermal subsidence and the sediment load both contribute to the geohistory subsidence, defined from stratigraphic analysis, with a relative impact of 60-65 % and 35-40 %, respectively.

From seismic profiles and their interpretation, stratigraphic modelling provides a way to either confirm or discard different hypothesis on subsidence. This method permits us to test hypothesis without some of the information needed for the "backstripping" method; for example lithological information is unnecessary. However, several assumptions, considered as reasonable in the case of our study area, have to be made, especially about the repetition of the sedimentary features (glacial erosion surfaces) through each glacial cycle. A future application of this technique will be to better constrain sediment supply. The European project PROMESS, which cored two boreholes on the outer shelf in 2004, will provide lithological and geochronological information for the last 500 ky sedimentary record. A new analysis at this time-scale will soon be undergone, taking into account the entire Gulf of Lions platform, in order to assess the space and time variability of the different components of subsidence.

6. Acknowledgements

This research is supported by the European Community through the PROMESS 1 (contract EVR1-CT–2002-40024) project, and from the Office of Naval Research. Additional support was provided by the French *Agence Nationale de la Recherche* (ANR, contract NT05-3-42040). Captains and crews of “Marion Dufresne”, “Le Suroît” and “L’Europe” are thanked for assistance during cruises “Images 5”, “Basar” 1 and 2, “Strataform”. The technical staffs of Genavir (data acquisition) and Ifremer/GM (data processing) are thanked. Researchers at the INSTAAR are thanked for their lively discussions on the stratigraphic simulations and subsidence analysis. Contribution number 1027 of the IUEM, European Institute for Marine Studies (Brest, France). Finally, we would like to thank Michael D. Blum for useful reviews that greatly improved the manuscript.

7. References

Airy, G.B., 1855. On the computation of the effect of the attraction of mountain-masses as disturbing the apparent astronomical latitude of stations of geodetic surveys. Philosophical Transaction of the Royal Society of London 145, 101-104.

Albertson, M.L., Dai, Y.B., Jensen, R.A., Hunter, R., 1950. Diffusion of submerged jets. American Society of Civil Engineers Transactions 115, 639-697.

Allen, P.A., Allen, J.R., 2005. Basin Analysis; Principles and Applications. Blackwell Publishing Ltd, Malden-Oxford-Victoria, 549 pp.

Aloïsi, J.C., 1986. Sur un modèle de sédimentation deltaïque: contribution à la connaissance des marges passives (Model of deltaic sedimentation: improve the knowledge on passive margins). Ph.D Thesis, Université de Perpignan, Perpignan, 162 pp.

Bassetti, M.A., Jouet, G., Dufois, F., Berné, S., Rabineau, M., Taviani, M., 2006. Sand bodies at the shelf edge in the Gulf of Lions (Western Mediterranean): deglacial history and modern processes. Marine Geology 234, 93-109.

Bentounsi, F., 1990. ECORS - Golfe du Lion. Interprétation des profils de sismique réflexion longue écoute - cinématique d'ouverture de la Méditerranée Occidentale (Geodynamic evolution of Western Mediterrnean based on the ECORS seismic profiles in the Gulf of Lions). M.Sc. Thesis, Université de Bretagne Occidentale, Brest, 69 pp.

Berné, S., Aloïsi, J.C., Baztan, J., Dennielou, B., Droz, L., Dos Reis, T., Lofi, J., Méar, Y., Rabineau, M., 2002. Notice de la carte morpho-bathymétrique du Golfe du Lion (Report on the mopho-bathymetric map of the Gulf of Lions). IFREMER and Région Languedoc Roussillon, Brest, 48 pp.

Berné, S., Lericolais, G., Marsset, T., Bourillet, J.F., de Batist, M., 1998. Erosional shelf sand ridges and lowstand shorefaces: examples from tide and wave dominated environments of France. Journal of Sedimentary Research 68(4), 540-555.

Bessis, F., 1986. Some remarks on the subsidence of sedimentary basins; application to the Gulf of Lions margin (western Mediterranean). Marine and Petroleum Geology 3(1), 37-63.

Bessis, F., Burrus, J., 1986. Etude de la subsidence de la marge du Golfe du Lion - Méditerranée occidentale (Subsidence of the Gulf of Lions margin in the Western Mediterranean). Bulletin Centre de Recherche Exploration-Production Elf Aquitaine 10, 123-141.

Biju-Duval, B., 1984. Les marges continentales françaises de la Méditerranée (French mediterranean continental margins). In: Boillot, G. (Ed.), Les marges Actuelles et Fossiles autour de la France. Masson, Paris, 249-334.

Burov, E.B., Diament, M., 1995. The effective elastic thickness (Te) of continental lithosphere: what does it really mean? Journal of Geophysical Research 100, 3905-3927.

Burrus, J., Audebert, F., 1990. Thermal and compaction processes in a young rifted basin containing evaporites: Gulf of Lions, France. American Association of Petroleum Geologists Bulletin 74(9), 1420-1440.

Burrus, J., 1984. Contribution to a geodynamic synthesis of the Provençal basin (North Western Mediterranean). Marine Geology 55, 247-269.

Ceramicola, S., Stoker, M., Praeg, D., Shannon, P.M., De Santis, L., Hoult, R., Hjelstuen, B.O., Laberg, S., Mathiesen, A., 2005. Anomalous Cenozoic subsidence along the `passive' continental margin from Ireland to mid-Norway. Marine and Petroleum Geology 22(9-10), 1045-1067.

Gensous, B., Tesson, M., 1996. Sequence stratigraphy, seismic profiles, and cores of Pleistocene deposits on the Rhône continental shelf. Sedimentary Geology 105, 183-190.

Gorini, C., Le Marrec, A., Mauffret, A., 1993. Contribution to the structural and sedimentary history of the Gulf of Lions (Western Mediterranean) from the ECORS profiles, industrial seismic profiles and well data. Bulletin de la Société Géologique de France 164(3), 353-363.

Got, H., 1973. Etude des corrélations tectonique-sédimentation au cours de l'histoire quaternaire du précontinent pyrénéo-catalan (Relative impacts of tectonic and sedimentary factors on the evolution of the Pyreneo-Catalan continent during Quaternary). Ph.D Thesis, Université de Perpignan, Université de Perpignan, 294 pp.

Gueguen, E., 1995. La Méditerranée Occidentale: un véritable océan (Genesis of the Western Mediterranean). Exemple de segmentation des marges et de hiatus cinématiques. Implications sur les processus d'amincissement crustal. Ph.D Thesis, Université de Bretagne Occidentale, Brest, 281 pp.

Huybrechts, P., 2002. Sea-level changes at the LGM from ice-dynamic reconstructions of the Greenland and Antarctic ice sheets during the glacial cycles. Quaternary Science Reviews 21, 203-231.

Huybrechts, P., de Wolde, J., 1999. The dynamic response of the Greenland and Antarctic ice sheets to multiple-century climatic warming. Journal of Climate 12, 2169-2188.

Johnston, P., 1995. The role of hydro-isostasy for Holocene sea-level changes in the British Isles. Marine Geology 124(1-4), 61-70.

Jouet, G., Berné, S., Rabineau, M., Bassetti, M.A., Bernier, P., Dennielou, B., Flores, J.A., Sierro, F.J., Taviani, M., 2006. Shoreface migrations at the shelf edge and sea-level changes around the Last Glacial Maximum (Gulf of Lions, NW Mediterranean). Marine Geology 234, 21-42.

Kirby, S.H., 1983. Rheology of the lithosphere. Reviews Geophysics and Space Physics 21, 1458-1487.

Lambeck, K., Bard, E., 2000. Sea-level changes along the French Mediterranean coast for the past 30,000 years. Earth and Planetary Science Letters 175, 203-222.

Lambeck, K., 1997. Sea-level change along the French Atlantic and Channel coasts since the time of the Last Glacial Maximum. Palaeogeography, Palaeoclimatology, Palaeoecology, 129(1-2), 1-22.

Lisitzin, E., 1974. Sea-Level Changes. Elsevier Oceanography Series, 8, Amsterdam-Oxford-New York, 286 pp.

Lofi, J., Rabineau, M., Gorini, C., Berné, S., Clauzon, G., De Clarens, P., Tadeu Dos Reis, A., Mountain, G.S., Ryan, W.B.F., Steckler, M.S., Fouchet, C., 2003. Plio-Quaternary prograding clinoform wedges of the western Gulf of Lion continental margin (NW Mediterranean) after the Messinian Salinity Crisis. Marine Geology 198(3-4), 289-317.

McKenzie, D.P., 1978. Some remarks on the development of sedimentary basins. Earth and Planetary Science Letters 40, 25-32.

Monaco, A., 1971. Contribution à l'étude géologique et sédimentologique du plateau continental du Roussillon (Geological and sedimentological framework of the continental shelf of the Roussillon). Ph.D Thesis, Université de Perpignan, Perpignan, 295 pp.

Paulson, A., Zhong, S., Wahr, J., 2005. Modelling post-glacial rebound with lateral viscosity variations. Geophysical Journal International 163, 357-371.

Peltier, W.R., 2004. Global glacial Isostasy and the surface of the ice-age earth: the ICE-5G (VM2) model and GRACE. Annual Review of Earth and Planetary Sciences 32, 111-149.

Peltier, W.R., 2002. On eustatic sea level history: Last Glacial Maximum to Holocene. Quaternary Science Reviews 21(1-3), 377-396.

Peltier, W.R., 1998. Postglacial variations in the level of the sea: implications for climate dynamics and solid-earth geophysics. Reviews of Geophysics 36, 603-689.

Plint, G.A., Nummendal, D., 2000. The falling stage systems tract: recognition and importance in sequence stratigraphic analysis. In: Hunt D., Gawthorpe, R.L. (Ed.), Sedimentary Responses to Forced Regressions. The Geological Society, London 1-17.

Posamentier, H.W., Jervey, M.T., Vail, P.R., 1988. Eustatic controls on clastic deposition I. Conceptual framework. In: Wilgus, C.K., Hastings, B.S., Kendall, C.G.S.C., Posamentier, H.W., Ross, C.A., Van Wagoner, J.C. (Ed.), Sea-Level Changes- an Integrated Approach. SEPM Spec. Pub. 42, Tulsa, 102-124.

Pratt, J.H., 1855. On the attraction of the Himalaya Mountains and of the elevated regions beyond them, upon the plumb line in India. Philosophical Transaction of the Royal Society of London 145, 53-100.

Rabineau, M., Berné, S., Aslanian, D., Olivet, J.L., Joseph, P., Guillocheau, F., Bourillet, J.F., Le Drezen, E., Granjeon, D., 2005. Sedimentary sequences in the Gulf of Lion: a record of 100,000 years climatic cycles. Marine and Petroleum Geology 22, 775-804.

Rabineau, M., 2001. Un modèle géométrique et stratigraphique des séquences de dépôts quaternaires de la plateforme du Golfe du Lion: enregistrement des cycles glacioeustatiques de 100 000 ans (Geometric and stratigraphic model of the quaternary depositional sequences of the Gulf of Lions platform). Ph.D Thesis, Université de Rennes 1, Rennes, (2 vols) 392 + 70 pp.

Sioni, S., 1997. Mer Ionienne et Apulie depuis l'ouverture de l'Océan Alpin (Evolution of Ionian Sea and Apulia from alpine oceanic openning). Ph.D Thesis, Université de Bretagne Occidentale, Brest, 208 pp.

Skene, K.I., Piper, D.J.W., Aksu, A.E., Syvitski, J.P.M., 1998. Evaluation of the global oxygen isotope curve as a proxy for Quaternary sea level by modelling of delta progradation. Journal of Sedimentary Research 68(6), 1077-1092.

Steckler, M.S., Mountain, G.S., Miller, K.G., Christie-Blick, N., 1999. Reconstruction of Tertiary progradation and clinoform development on the New Jersey passive margin by 2-D backstripping. Marine Geology 154(1-4), 399-420.

Steckler, M.S., Watts, A.B., 1980. The Gulf of Lion: subsidence of a young continental margin. Nature 287, 425-429.

Syvitski, J.P., Hutton, E.W.H., 2001. 2D SEDFLUX 1.0C: an advanced process-response numerical model for the fill of marine sedimentary basins. Computers & Geosciences 27(6), 731-753.

Syvitski, J.P.M., Nicholson, M., Skene, K., Morehead, M.D., 1998. PLUME1.1: Deposition of sediment from a fluvial plume. Computers & Geosciences 24(2), 159-171.

Syvitski, J.P.M., 1989. The process-response model in Quantitative Dynamic Stratigraphy. In: Cross, T.A. (Ed.), Quantitative Dynamic Stratigraphy. Prentice-Hall, New York, 309-334.

Tesson, M., Posamentier, H., Gensous, B., 2000. Stratigraphic organisation of Late Pleistocene deposits of the western part of the Rhone shelf (Languedoc shelf) from high resolution seismic and core data. American Association of Petroleum Geologists Bulletin 84(1), 119-150.

Tesson, M., Gensous, B., Allen, G.P., Ravenne, C., 1990. Late Quaternary lowstand wedges on the Rhône Continental Shelf, France. Marine Geology 91, 325-332.

Turcotte, D.L., Schubert, G., 1982. Geodynamics, Applications of Continuum Physics to Geological Problems. John Wiley & Sons, New York, 450 pp.

Van Hinte, J.E., 1978. Geohistory analysis: application of micropaleontology in exploration geology. Bulletin American Association of Petroleum Geologists 62, 201-222.

Waelbroeck, C., Labeyrie, L.D., Michel, E., Duplessy, J.-C., McManus, J., Lambeck, K., Balbon, E., Labracherie, M., 2002. Sea-level and deep water changes derived from benthic Foraminifera isotopic record. Quaternary Science Reviews 21(1-3), 295-305.

Watts, A.B., 2001. Isostasy and Flexure of the Lithosphere, Cambridge University Press, Cambridge, 458 pp.

Watts, A.B., 1992. The effective elastic thickness of the lithosphere and the evolution of foreland basin. Basin Research 4, 169–178.

Watts, A.B., Karner, G.D., Steckler, M.S., 1982. Lithospheric flexure and the evolution of sedimentary basins. Philosophical Transaction of the Royal Society of London 305 Series A, 249-281.

Watts, A.B., Ryan, W.B.F., 1976. Flexure of the lithosphere and continental margin basins, Tectonophysics 36, 25-44.

8. Figure captions

Fig. 1: Definition of mechanisms causing subsidence on a passive continental margin. Total subsidence (*S*) results from vertical motions that are specific for each lithology. Different subsidence components can be determined by mechanisms that cause these motions. Note term geohistory subsidence (*GS*) that corresponds to subsidence measured from seismic stratigraphy and associated to combination of tectonic/thermal subsidence (*TS*) and sediment load (*SL*).

Fig. 2: Flow chart of method defined in this paper and aimed at investigating different components of total subsidence (*S*). Strategy uses stratigraphic modelling along with *Sedflux* program and input parameters from geohistory and stratigraphic analysis.

Fig. 3: Gulf of Lions continental margin (North-Western Mediterranean); Geographic, morpho-bathymetric (from Berné *et al*., 2002) and hydrographic settings. Dotted line indicates position of NE–SW seismic synthesis shown on figure 4. Location of North-South simulated profile on map shows that marine section presented here is between 50 and 130 km. Note that simulations take into account entire profile (including onshore section).

Fig. 4: Stratigraphic interpretation from composite high-resolution Sparker seismic lines (position in Fig. 3). NE–SW transect across platform illustrates stacking of last five sedimentary sequences (S1 to S5) bounded by major discontinuities (D40 to D70). Within these sequences, deposits are organized in a vertically stacked sedimentary motif consisting of prisms (PI) with gently dipping clinoforms, and prisms (PII) with relatively high-angle

clinoforms (from 3 to 7°) (Rabineau *et al*, 2005). Highest amplitude seismic reflections reveal major erosional surfaces that formed during overall sea-level fall and lowstands.

Fig. 5: Chirp seismic profile across continental shelf (position in Fig. 3). Major seismic surfaces correspond to cyclic erosion surfaces formed during forced regressions (see text for detailed explanation).

Fig. 6: Definition of geohistory subsidence (*GS*) and water loading (*WL*) as they are input in numerical stratigraphic model *Sedflux*. Identification of dated erosion paleosurfaces permits one to quantify their vertical evolution through time, and to estimate *GS* subsidence. This value takes into account both tectonic subsidence (*TS*) and loads due to sediment deposition (*SL*). Water loading (*WL*) results from relative sea-level fluctuations and reaches its maximum between glacial and interglacial periods.

Fig. 7: Test of isostatic parameters used in numerical stratigraphic model *Sedflux*. Total subsidence (*S*) is modelled using different values of **1**- effective elastic thickness (EET) and **2**- relaxation time (RT).

Fig. 8: 1- Modelling of total subsidence (*S*) with best adapted isostatic parameters (Model R8: EET = 65 km; RT = 3,500 years). **2-** Evolution through time of *GS*, *S* and *WL* subsidence from this simulation R8.

Fig. 9: Modelling of total subsidence (*S*) and (*S'*). (*S'*) is results of Model R9 with sediment flux turned on. Comparison of these models permits estimation of different components of total subsidence (*S*) at 100 km of simulated section (outer shelf).

Table 1: Description of different numerical stratigraphic models (R1 to R9) and their input parameters.

Table 2: Quantification of different components of total subsidence (*S*) at 100 and 120 km of simulated section.

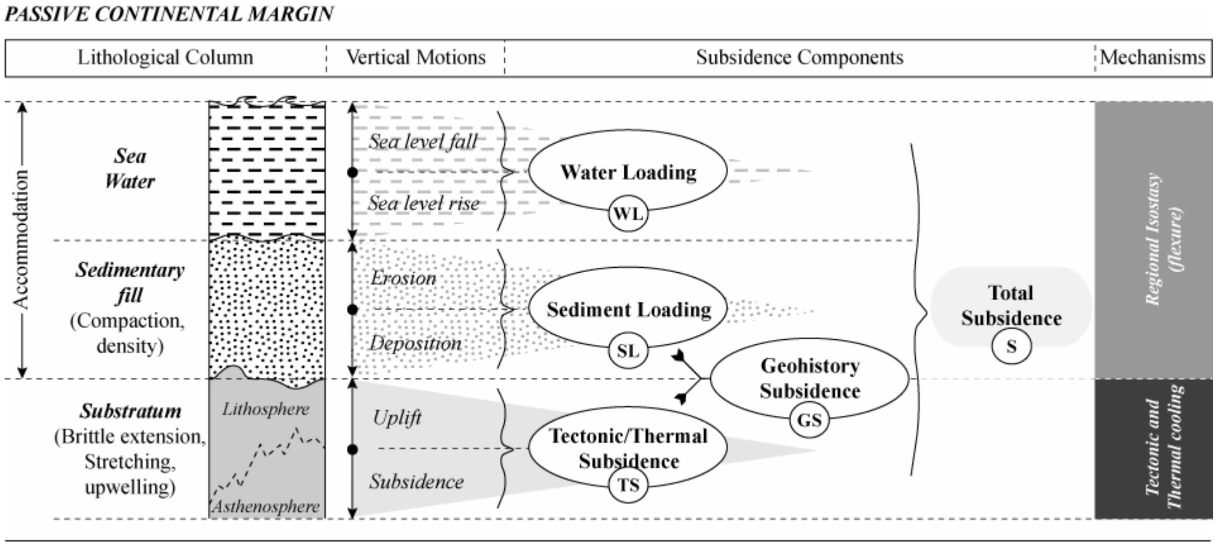

Figure. 1 - Jouet *et al.*

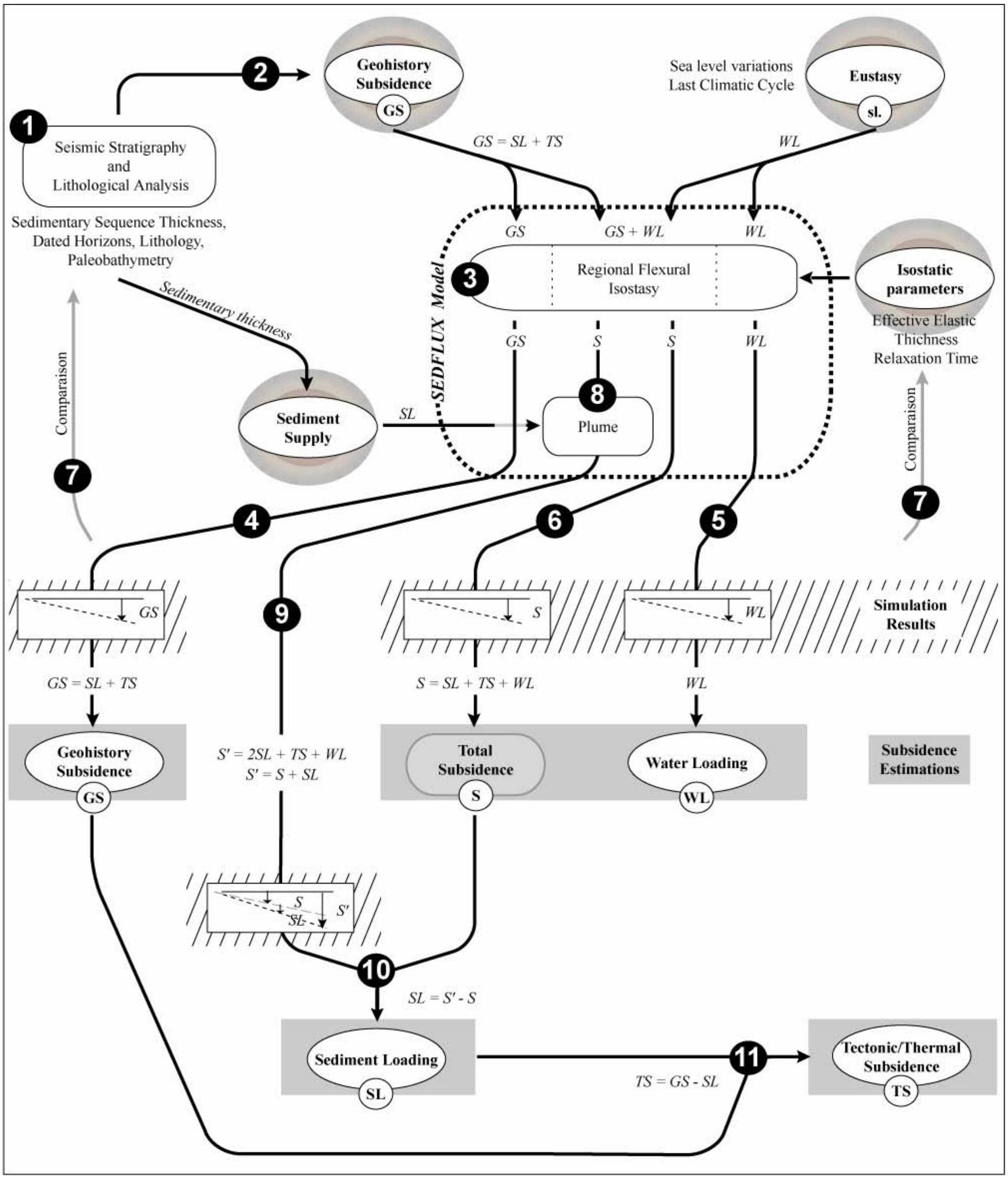

Figure. 2 - Jouet *et al.*

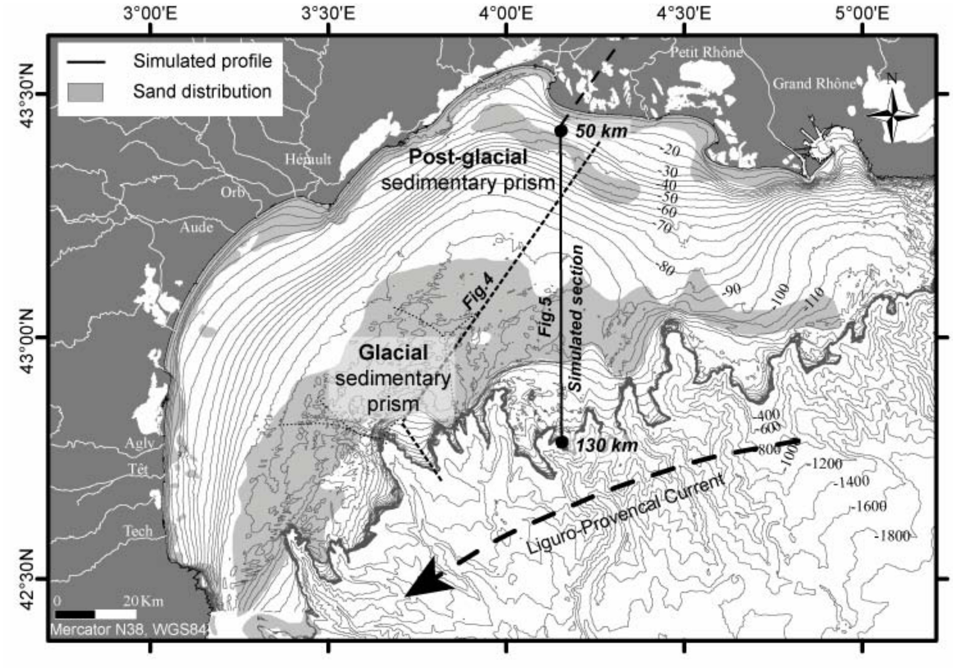

Figure. 3 - Jouet *et al.*

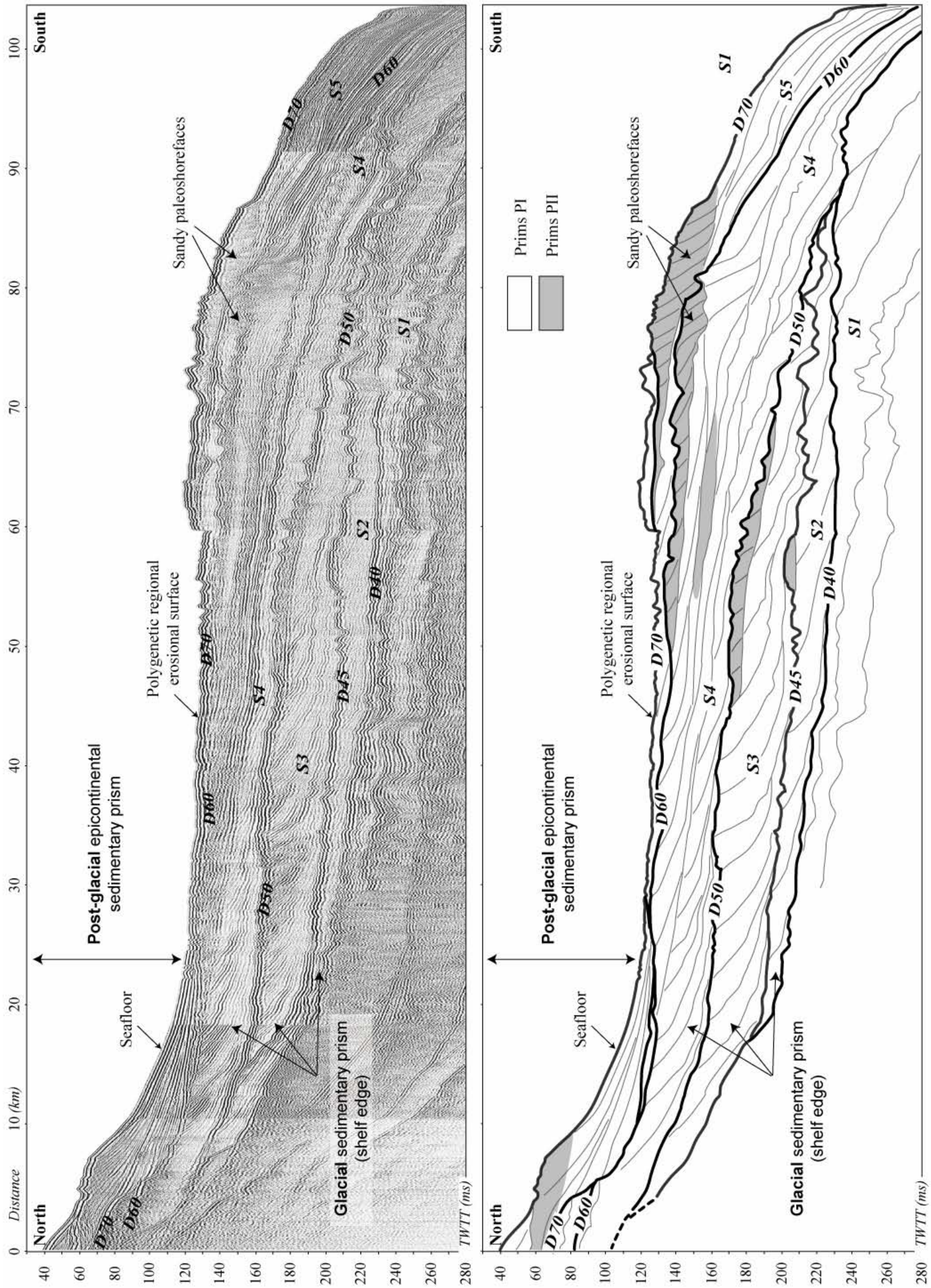

Figure. 4 - Jouet *et al.*

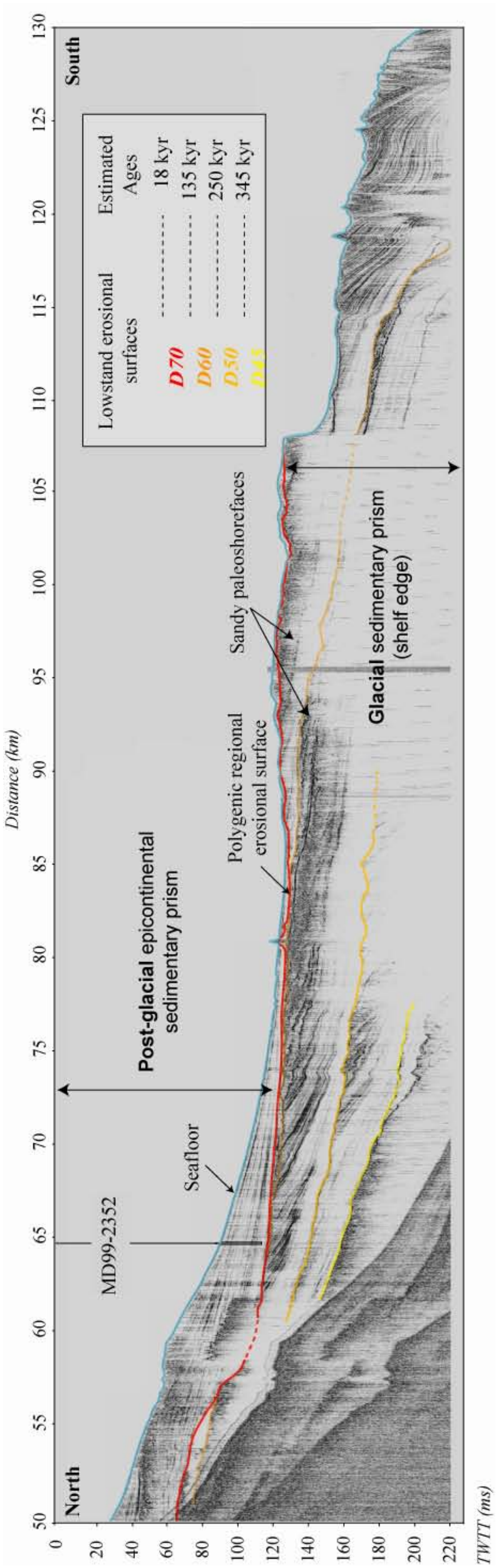

Figure. 5 - Jouet *et al.*

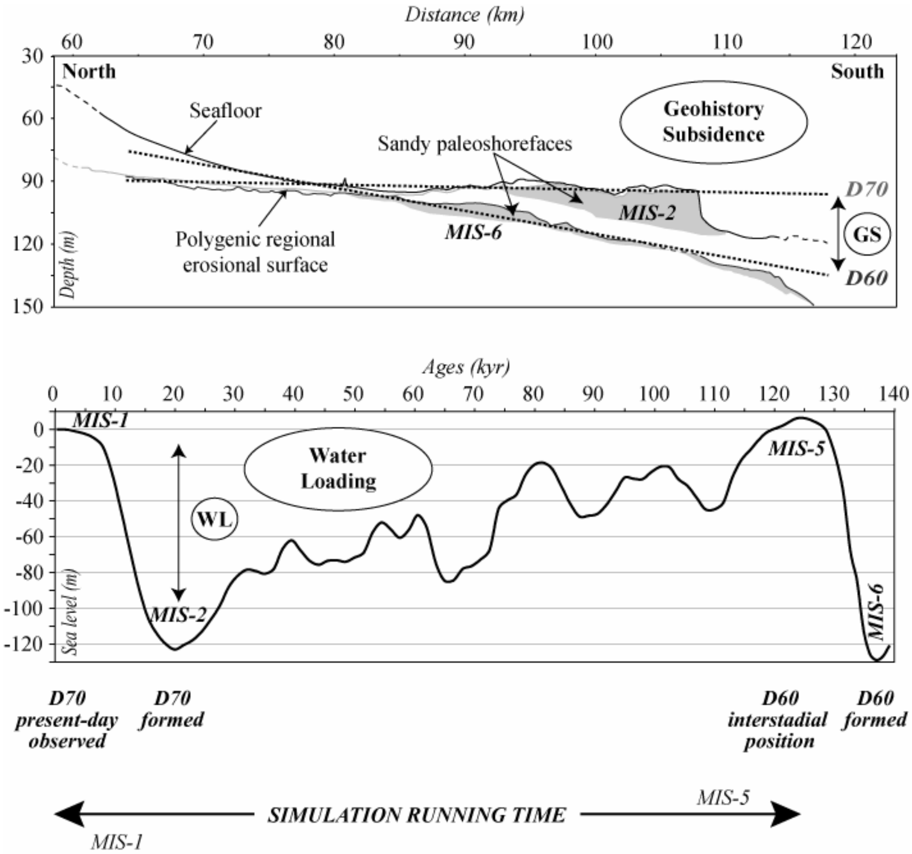

Figure. 6 - Jouet *et al.*

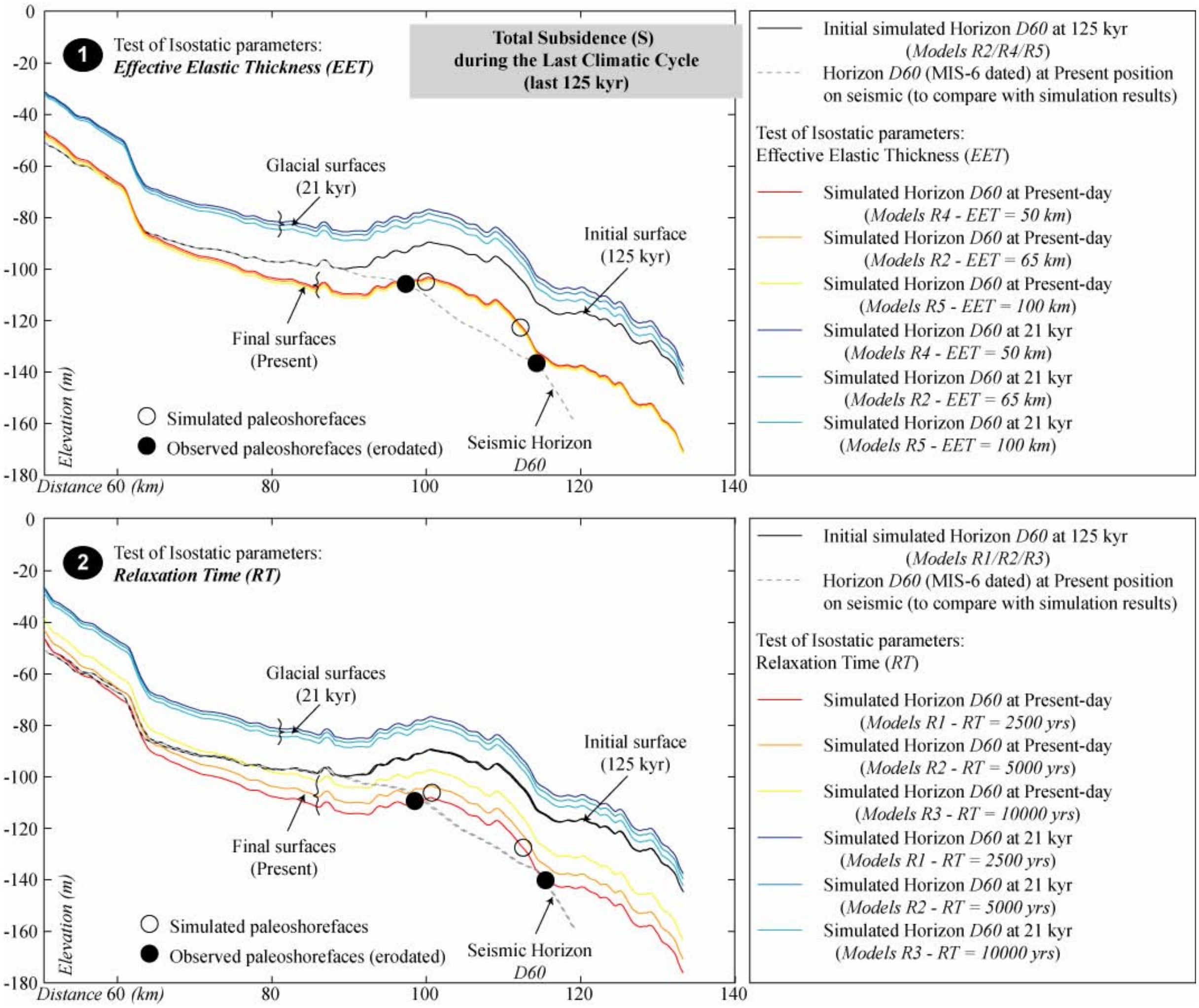

Figure. 7 - Jouet *et al.*

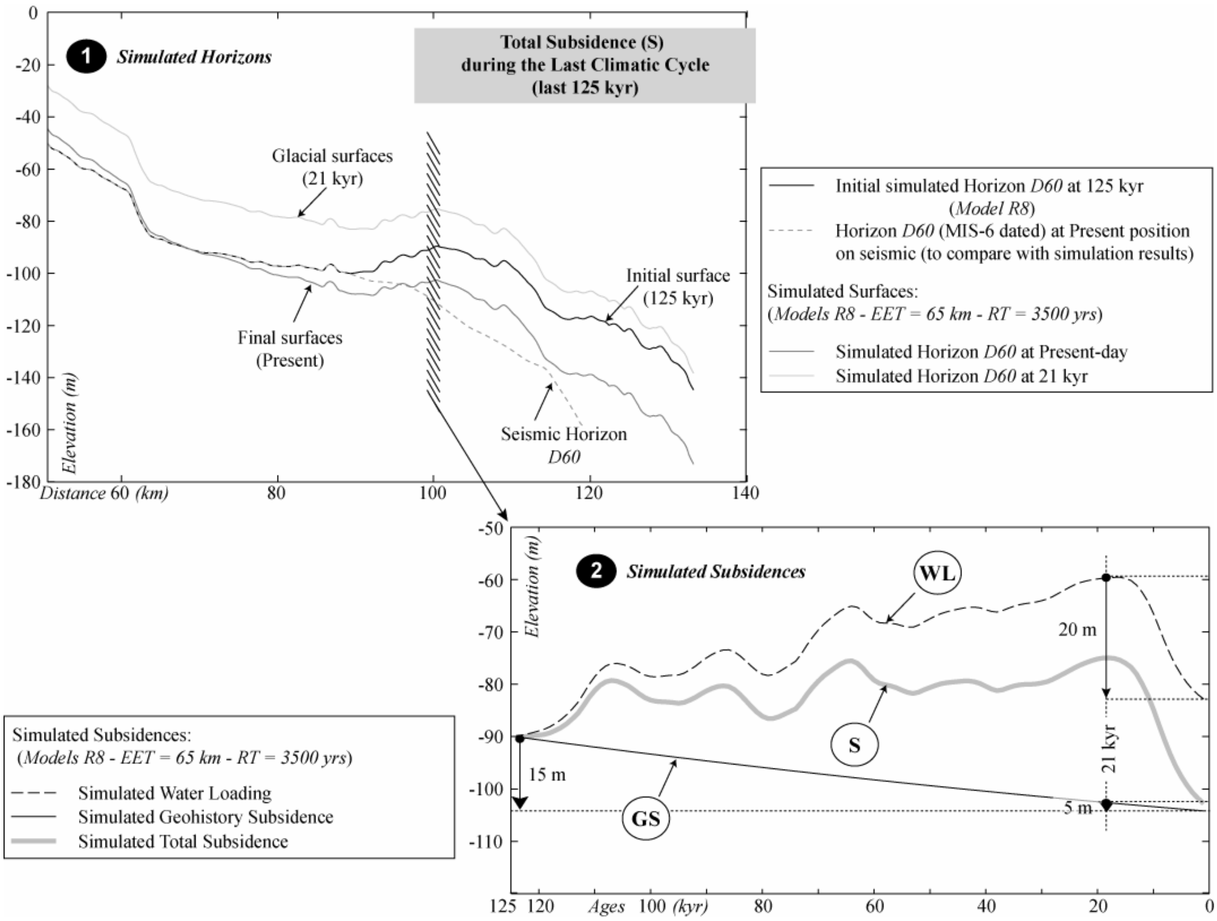

Figure. 8 - Jouet *et al.*

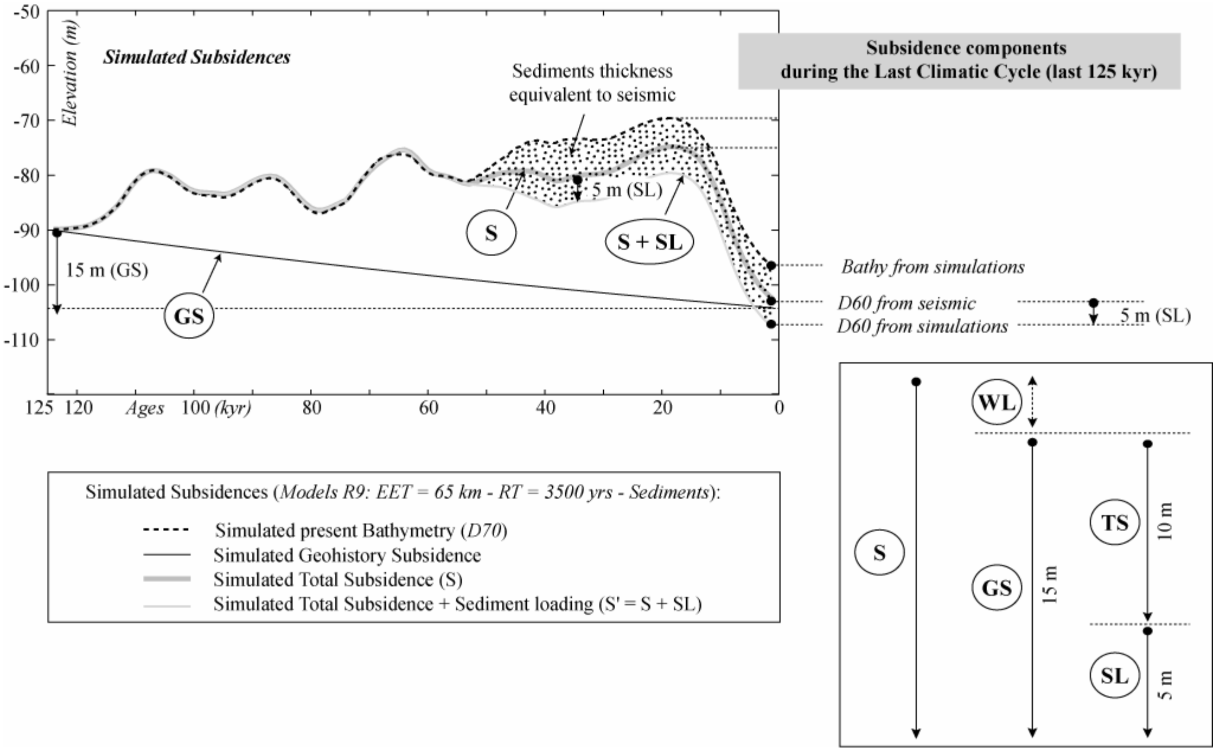

Figure. 9 - Jouet *et al.*

MODELS	DESCRIPTION	ISOSTASY		SUBSIDENCE		SEDIMENT	DURATION
		Isostatic Effective Elastic Thickness (km)	*Isostatic Relaxation Time (yrs)*	*Inner shelf (m/yrs)*	*Outer shelf (m/yrs)*		
R1	Fast margin adjustment	65	2 500	0 (50 km)	2,5E-04	No	LCC (125 kyr)
R2	Medium margin adjustment	65	5 000	0 (50 km)	2,5E-04	No	LCC (125 kyr)
R3	Slow margin adjustment	65	10 000	0 (50 km)	2,5E-04	No	LCC (125 kyr)
R4	Local margin adjustment	50	5 000	0 (50 km)	2,5E-04	No	LCC (125 kyr)
R5	Regional margin adjustment	100	5 000	0 (50 km)	2,5E-04	No	LCC (125 kyr)
R6	Conv. point migration, fast adjustment	65	2 500	0 (50-80 km)	2,5E-04	No	LCC (125 kyr)
R7	Conv. point migration, medium adjustment	65	5 000	0 (50-80 km)	2,5E-04	No	LCC (125 kyr)
R8	Adapted eath model (LCC)	65	3 500	0 (50-80 km)	2,5E-04	No	LCC (125 kyr)
R9	Estimation of the Sediment load	65	3 500	0 (50-80 km)	2,5E-04	Yes	LCC (125 kyr)

Table. 1 - Jouet *et al.*

MODELS	DESCRIPTION	POSITION 100 km						
		Total Subsidence LCC D60 (m)	*Sediment Thickness D60-D70 (m)*	*Total Subsidence LD D70 (m)*	*Subsidence (Sed. Load. + Teconics) (m)*	*Hydo-Isostasy (Water Load.) (m)*	*Sediment Loading (m)*	*Tectonic Subsidence (m)*
	- At position 100 km -							
R8	Adapted eath model (LCC)	+15	+10	+25	+4,5	+20,5		
R9	Estimation of the Sediment load						1/3 Subsid	2/3 Subsid
	- At position 120 km -							
R8	Adapted eath model (LCC)	+10	+15	+25	+5,5	+19,5		
R9	Estimation of the Sediment load						1/3 Subsid	2/3 Subsid

Table. 2 - Jouet *et al.*